Available online at www.sciencedirect.com

ScienceDirect

IFAC PapersOnline CONFERENCE PAPER ARCHIVE

IFAC PapersOnLine 55-21 (2022) 102–107

Observable Dynamic Models of Reagent Effects for Model-based Froth Flotation Control ⋆

Jaco-Louis Venter * **Johan D. Le Roux** *,1 **Ian K. Craig** *

* *Department of Electrical, Electronic and Computer Engineering, University of Pretoria, Pretoria, South Africa.*

Abstract: This article demonstrates the feasibility of including simple reagent addition models in an existing observable dynamic model of a froth flotation circuit. The existing model has full state observability and parameter identifiability using measurements that are commonly available on flotation circuits. This article qualitatively evaluates the possible impact of varying frother dosage on the model parameters. A Sobol sensitivity analysis indicates that the air recovery model parameters are most influential in the determination of grade and recovery. The model is expanded with two different reagent effect models. Both expansions include mass balance models of the frother concentration in each cell. The first model expands an empirical parameter in the air recovery model, related to the froth height at which peak air recovery (PAR) is achieved, as a linear function of frother concentration. The second model adds a linear frother concentration term to the existing air recovery model to modify the steady-state air recovery directly. Observability analyses of the expanded models show that all states and the important time-varying model parameters are observable (and identifiable) from the available on-line measurements. Most importantly, the frother concentrations are shown to be observable without concentration measurements. Simulations of the model expansions show that the second model can qualitatively predict the impact of increased frother dosage on air recovery, grade, and recovery, while the first model can only predict the correct effect under certain conditions.

Keywords: Froth flotation, frother, observability, Sobol sensitivity analysis, reagent model

1. INTRODUCTION

Significant research effort has been dedicated to understand and control flotation since its development in the 1890s as a mineral separation technique. The scale of flotation utilisation means that even slight improvements in efficiency could have a large impact on the global minerals processing industry (Quintanilla et al., 2021a). Of the operating parameters involved in flotation circuits, the reagents and their dosages are especially important (Harris et al., 2013). Reagents affect true flotation, entrainment, and froth stability significantly, even though they are typically added in very small quantities. These phenomena are commonly identified in literature as the most important mechanisms that determine grade and recovery (Oosthuizen et al., 2021; Quintanilla et al., 2021a; Steyn and Sandrock, 2021; Wills and Finch, 2015).

Recent models specifically aim at the development of model-based control strategies for the flotation process (Oosthuizen et al., 2021; Quintanilla et al., 2021a; Steyn and Sandrock, 2021; Shean et al., 2018). The control of froth flotation is especially challenging due to severely limited process measurements (Oosthuizen et al., 2017; Shean and Cilliers, 2011) and complex interactions in the flotation process which are not yet fully understood, such as the dynamics in the froth phase (Quintanilla et al., 2021b). In this regard, the model developed by Oosthuizen et al. (2021) is especially promising. By developing a semi-mechanistic model with observable states and parameters that are identifiable from typically available on-line measurements, poorly understood processes do not need to be modelled phenomenologically. Instead, state-estimation can update the parameters in real time to expand the long-term accuracy and operating range of the model (Oosthuizen et al., 2021).

A model-based control strategy that includes reagent addition as a manipulated variable (MV) requires explicit modelling of reagent effects – which is not included in the Oosthuizen et al. (2021) model. According to the knowledge of the authors, the explicit modelling of reagent effects are also not available in other recently developed dynamic models (Quintanilla et al., 2021a; Steyn and Sandrock, 2021). Furthermore, only a handful of older models include such considerations to a some degree (Casali et al., 2002; Hodouin et al., 2000; Maldonado et al., 2010; Putz and Cipriano, 2015).

The purpose of this work is to expand on the utility of the Oosthuizen et al. (2021) by adding simple reagent addition models to it for use in model-based control strategies. Only a brief overview of the model by Oosthuizen et al. (2021) is given, with an emphasis on which parameters could be affected by changing reagent concentrations. For

⋆ This work is based on research supported in part by the National Research Foundation of South Africa (Grant Number: 137769)

[1] Corresponding author, E-mail: derik.leroux@up.ac.za

10.1016/j.ifacol.2022.09.251

the purpose of this study, only the effect of collectors and frothers are considered. These are the two most common reagent types (Wills and Finch, 2015) and their impact is often studied experimentally, albeit in most cases without the development of an accompanying model (Casali et al., 2002; Finch et al., 2008; Maldonado et al., 2010; Putz and Cipriano, 2015; Wang et al., 2017; Wiese et al., 2011).

A Sobol sensitivity analysis is used to identify the most important parameters for grade and recovery prediction. Guided by the sensitivity results, two model expansions of the air recovery model in Oosthuizen et al. (2021) are proposed. Their state observability and parameter identifiability (Villaverde et al., 2019) are analysed given measurements generally available at a flotation plant. Qualitative simulations are used to judge how appropriate the expansions are.

2. EXISTING MODELLING FRAMEWORK

2.1 Model Description

Oosthuizen et al. (2021) models each mechanical cell (subscript k), and hopper (subscript H) in a flotation bank (see Fig. 1) individually, and considers any number of mineral species (superscript i) and mineral classes (superscript j). The cell and hopper levels (L_k and L_H) are modelled using simple volume balances with the initial volumetric feed (Q_{F_1}) considered a measured disturbance and the tailings flow-rates (Q_{T_k}), and hopper outflow (Q_H) taken as MVs.

The concentrate volumetric flow-rate (Q_{C_k}) is calculated from the superficial gas velocity (J_{g_k}), air recovery (α_k), top of froth bubble size (D_{BF_k}), and fluid properties using the model developed by Neethling and Cilliers (2003). The model makes use of the Plateau border drag coefficient (C_{PB}), which is one of the parameters Oosthuizen et al. (2021) estimates from the plant measurements.

The mineral masses in the cells ($M_k^{i,j}$), are modelled using simple mass balances that assume a well-mixed pulp phase. The mass flow-rates leaving a cell in the concentrate ($\dot{M}_{C_k}^{i,j}$) are calculated as

$$\dot{M}_{C_k}^{i,j} = K^{i,j} M_k^{i,j} S_{b_k} \alpha_k + Ent_{Frac}^{i,j} \frac{M_k^{i,j}}{L_k A_k} Q_{C_k}, \quad (1)$$

where A_k is the cell cross-sectional area, $K^{i,j}$ is the flotation rate constant and the bubble surface area flux (S_{b_k}) is

$$S_{b_k} = 6 \frac{J_{g_k}}{D_{BP_k}}. \quad (2)$$

Oosthuizen et al. (2021) takes the pulp bubble diameter (D_{BP_k}) as a constant parameter with value 0.6 mm.

The second term in (1) quantifies recovery via entrainment using a simplified version of the entrainment factor ($Ent_{Frac}^{i,j}$) model developed by Neethling and Cilliers (2009). The entrainment depends on the minimum and maximum particle diameters of all modelled particle sizes ($d_{p,\min}$ and $d_{p,\max}$), the fluid properties (including C_{PB}), α_k, J_{g_k}, and froth height (h_{f_k}). The froth height is taken as the difference between the cell depth (H_{cell}) and L_k.

The top of froth bubble size and air recovery are modelled as

$$\frac{\mathrm{d}D_{BF_k}}{\mathrm{d}t} = \frac{K_{BS_{J_g}} J_{g_k} + K_{BS_\lambda} \lambda_{\text{air}_k} - D_{BF_k}}{\lambda_{\text{air}_k}}, \quad (3)$$

$$\begin{aligned} \frac{\mathrm{d}\alpha_k}{\mathrm{d}t} =& \frac{K_{\alpha_{J_g}} \left(J_{g_k} - K_{0,\alpha_{J_g}} \right)^2}{\lambda_{\text{air}_k}} \\ &+ \frac{K_{\alpha_{h_f}} \left(h_{f,k} - K_{0,\alpha_{h_f}} \right)^2 - \alpha_k}{\lambda_{\text{air}_k}}, \end{aligned} \quad (4)$$

where λ_{air_k} is a measure of the froth residence time

$$\lambda_{\text{air}_k} = \frac{h_{f_k}}{J_{g_k}}. \quad (5)$$

The parameters $K_{BS_{J_g}}$, K_{BS_λ}, $K_{\alpha_{J_g}}$, $K_{\alpha_{h_f}}$, $K_{0,\alpha_{J_g}}$, and $K_{0,\alpha_{h_f}}$ characterise the effects of J_{g_k} and λ_{air_k} (alternatively h_{f_k}) on D_{BF_k} and α_k. The values of $K_{\alpha_{J_g}}$ and $K_{\alpha_{h_f}}$ are fitted to steady-state experimental data, and are assumed to remain constant. It is known that changes in both h_{f_k} and J_{g_k} result in peaks in air recovery (PAR) (Hadler et al., 2012). Oosthuizen et al. (2021) models this behaviour with inverted parabolas in (4). The $K_{0,\alpha_{J_g}}$, and $K_{0,\alpha_{h_f}}$ parameters correspond to the values of J_{g_k} and h_{f_k} for which PAR is achieved.

Along with C_{PB} and $K^{i,j}$, the parameters $K_{BS_{J_g}}$, K_{BS_λ}, $K_{0,\alpha_{J_g}}$, and $K_{0,\alpha_{h_f}}$ are to be estimated from the available on-line measurements: L_k, L_H, D_{BF_k}, α_k, hopper grade (G_H), total mass flow from the hopper ($\dot{M}_H^{\text{Tot}}$), total final tailings mass flow-rate ($\dot{M}_{T_f}^{\text{Tot}}$), and the final tailings grade (G_T).

2.2 Impact of Reagents

Collectors are used to preferentially enhance the floatability of the desired mineral, but can also increase the floatability of gangue if used in excess (Wills and Finch, 2015). Wiese et al. (2011) have shown that changes in bubble loading due to collector variations can also have an impact on froth stability. However, for this study the collector concentration is assumed to mainly impact the floatability rate constants, $K^{i,j}$.

Frother addition is aimed at reducing the pulp bubble size and improving froth formation and stability (Harris et al., 2013; Wills and Finch, 2015). Increasing the frother dosage only reduces D_{BP_k} up to a point known as the critical coalescence concentration (CCC), beyond which D_{BP_k} remains a function of the aeration rate and dispersion mechanism (Finch et al., 2008; Harris et al., 2013; Wills and Finch, 2015). While the frother dosage typically surpasses the CCC (Harris et al., 2013), and D_{BP_k} is not expected to vary much, it is included in the sensitivity analysis in Section 3 for completeness.

The effects of frother dosage on froth stability would likely be modelled best as part of the D_{BF_k} and α_k state equations (see (3) and (4)), as these states are related to the rates of bubble coalescence, bursting and froth structure (Oosthuizen et al., 2021). Unfortunately, due to the empirical nature of some of the parameters in these equations ($K_{BS_{J_g}}$, K_{BS_λ}, $K_{\alpha_{J_g}}$, $K_{\alpha_{h_f}}$, $K_{0,\alpha_{J_g}}$ and $K_{0,\alpha_{h_f}}$) and the lack of experimental data with varying reagent dosages for the simulated circuit, it is difficult to

determine which of these parameters would change with reagent concentration and to what extent.

The Plateau border drag coefficient is also considered. Together with D_{BF_k} and α_k, C_{PB} plays a role in determining the water recovery, Q_{C_k}, and entrainment of particles (Neethling and Cilliers, 2009; Oosthuizen et al., 2021). For the purpose of this study, C_{PB} will be considered in the sensitivity analysis as being affected by the frother concentration.

3. SENSITIVITY ANALYSIS

The Sobol sensitivity analysis is a global variance-based sensitivity analysis method that quantifies the relative contribution of the variance in each input factor, X_i, to the total variance in the model output Y (Saltelli et al., 2010). The contribution is quantified by first-order and total sensitivity indexes (S_i and S_{Ti}). The value of S_i is the fraction of the variance in Y that can be attributed to the variation of X_i alone, while S_{Ti} is the fraction of variance in Y that can be attributed to any joint factor variation that includes X_i (Saltelli et al., 2010). The indexes are given as

$$S_i = \frac{\mathrm{V}_{X_i}\left(\mathrm{E}_{\mathbf{X}_{\sim i}}\left(Y|X_i\right)\right)}{\mathrm{V}(Y)}, \tag{6}$$

$$S_{Ti} = \frac{\mathrm{E}_{\mathbf{X}_{\sim i}}\left(\mathrm{V}_{X_i}\left(Y|\mathbf{X}_{\sim i}\right)\right)}{\mathrm{V}(Y)}, \tag{7}$$

where E and V respectively denote the expected value and variance operators, and $\mathbf{X}_{\sim i}$ denotes the matrix of all factors except for X_i. The $\mathrm{V}_{X_i}\left(\mathrm{E}_{\mathbf{X}_{\sim i}}\left(Y|X_i\right)\right)$ term in (6) is the variance in the mean of Y, with all factors except X_i varied, taken over the entire range of X_i. The $\mathrm{E}_{\mathbf{X}_{\sim i}}\left(\mathrm{V}_{X_i}\left(Y|\mathbf{X}_{\sim i}\right)\right)$ term in (7) is the expected variance of Y, with all factors except X_i fixed. Saltelli et al. (2010) discuss how each of these sensitivity indexes can be calculated from function evaluations in a Monte-Carlo simulation and the use of the Sobol sequence, a low-discrepancy quasi-random sampling method that aims to sample the input factor space more completely.

The parameters considered as input factors, their nominal values and sensitivity indexes for steady-state grade and recovery are summarised in Table 1. Only two mineral groups were considered: the desired mineral, $\{0, 0\}$, and gangue, $\{1, 0\}$. Ideally, each parameter should be varied over the full range that can be achieved by varying the reagent concentrations by a given amount. In the absence of data on parameter values over a larger operating range or other reagent concentrations, it is very difficult to specify realistic ranges over which to carry out the sensitivity analysis. For the purpose of the current study, aimed at showing the feasibility of this approach, the parameters were all allowed to vary by 10 % of their nominal value, based on plant data in Hadler et al. (2010).

There is a large difference in the concentrations of the desired mineral and gangue (typically the desired mineral mass fraction in a cell is less than about 0.015). The desired mineral floatability constant ($K^{0,0}$) is also much larger than that of the gangue ($K^{1,0}$). These factors result in true flotation dominating the recovery of desired mineral in the concentrate ($\dot{M}^{0,0}_{C_k}$) and entrainment dominating the mass flow rate of gangue in the concentrate ($\dot{M}^{1,0}_{C_k}$). As the recovery is mostly determined by true flotation, it is expected to be sensitive only to factors that influence true flotation. The grade will additionally be influenced by all factors that have an impact on entrainment.

According to Table 1, the parameter with the highest sensitivity for both grade and recovery determination is $K_{0,\alpha_{h_f}}$, followed by $K_{0,\alpha_{J_g}}$. This implies that air recovery is probably the dominating factor in the water recovery, entrainment and flotation models. While C_{PB}, $K_{BS_{J_g}}$, and K_{BS_λ} were the next most important for grade, they had no real impact on recovery as they only affect entrainment directly. The grade sensitivity towards C_{PB} warrants future investigation into the impact reagents might have on this parameter. The sensitivity indexes for $K^{1,0}$, $K_{\alpha_{J_g}}$ and $K_{\alpha_{h_f}}$ were small enough to justify assuming constant values for these parameters.

4. FROTHER MODEL

The model of Oosthuizen et al. (2021) is expanded in Sections 4.1 and 4.2 to explicitly account for reagent effects. The observability and identifiability of the model expansions were evaluated by calculating the rank of the observability matrix ($\mathcal{O}$) for a linearised version of the model with parameters considered constant state variables (Villaverde et al., 2019). This is a sufficient (although not necessary) condition for the observability of a non-linear system (Hermann and Krener, 1977). Although not used in the observability analysis by Oosthuizen et al. (2021), the frother addition rate to the first cell ($\dot{M}^f_{F_1}$) is assumed to be measured on-line and will be used in the current observability analysis. The manipulated variables are: J_{g_k}, Q_{T_k}, Q_H and $\dot{M}^f_{F_1}$. The available measurements are: L_k, L_H, D_{BF_k}, α_k, G_H, $\dot{M}^{\mathrm{Tot}}_H$, G_T, and $\dot{M}^{\mathrm{Tot}}_{T_f}$.

The frother mass in each cell (M^f_k) was modelled using simple mass balances

$$\frac{\mathrm{d}M^f_k}{\mathrm{d}t} = \dot{M}^f_{F_k} - C^f_k(Q_{T_k} + Q_{C_k}), \tag{8}$$

where the frother mass in-flow rate ($\dot{M}^f_{F_k}$) will typically be the out-flow rate from the previous cell. The exception is the first cell in the bank, where $\dot{M}^f_{F_1}$ is an additional MV. This assumes that the frother leaves the cell in the concentrate and tailings based on the concentration in the pulp, C^f_k, which is

Table 1. Sensitivity indexes (in percentage)

Parameter	Nominal value	Grade		Recovery	
		S_1	S_T	S_1	S_T
C_{PB}	12.0	13.0	13.4	0.0	0.0
D_{BP_k}	0.6 mm	0.9	1.2	5.1	5.1
$K^{0,0}$	2.3	1.5	1.7	5.0	5.1
$K^{1,0}$	2.14×10^{-4}	0.0	0.0	0.0	0.0
$K_{0,\alpha_{J_g}}$	8.42	23.3	23.7	14.5	16.7
$K_{0,\alpha_{h_f}}$	94.9	49.3	49.8	70.7	74.6
$K_{\alpha_{J_g}}$	-1.9×10^{-2}	0.1	0.4	0.8	0.4
$K_{\alpha_{h_f}}$	-1.0×10^{-4}	0.9	1.2	1.8	2.5
$K_{BS_{J_g}}$	0.067	6.2	6.7	0.0	0.0
K_{BS_λ}	0.032	3.4	3.4	0.0	0.0

$$C_k^f = \frac{M_k^f}{L_k A_k}. \tag{9}$$

As the most influential parameters identified in the sensitivity analysis ($K_{0,\alpha_{hf}}$ and $K_{0,\alpha_{J_g}}$) are primarily influenced by the frother, the collector concentrations were not modelled.

4.1 Model Expansion 1 (ME1)

At first a simple linear expansion

$$K_{0,\alpha_{hf},k} = K_{CF} C_k^f + K_{CF,0}, \tag{10}$$

of the most important parameter, $K_{0,\alpha_{hf}}$, was investigated. Here K_{CF} quantifies the impact of C_k^f on $K_{0,\alpha_{hf}}$ and $K_{CF,0}$ is the value of $K_{0,\alpha_{hf}}$ when the frother concentration is 0.

If $K_{CF,0}$ is assumed to be constant, all states (including frother concentrations (C_k^f)) are observable and all estimated parameters (C_{PB}, $K^{i,j}$, $K_{0,\alpha_{J_g}}$, $K_{BS_{J_g}}$, K_{BS_λ}, and K_{CF}) are identifiable from the available measurements and known MVs.

4.2 Model Expansion 2 (ME2)

A more appropriate expansion (which considers process knowledge) modifies the steady-state value of α_k by adding $K_{F\alpha}(C_k^f - K_{F\alpha,0})$ to the numerator of (4)

$$\frac{\mathrm{d}\alpha_k}{\mathrm{d}t} = \frac{K_{\alpha_{J_g}}\left(J_{g_k} - K_{0,\alpha_{J_g}}\right)^2 + K_{\alpha_{h_f}}\left(h_{f,k} - K_{0,\alpha_{hf}}\right)^2}{\lambda_{\mathrm{air}_k}} + \frac{K_{F\alpha}(C_k^f - K_{F\alpha,0}) - \alpha_k}{\lambda_{\mathrm{air}_k}}. \tag{11}$$

The frother concentrations (C_k^f) remain observable and both of the additional parameters ($K_{F\alpha}$ and $K_{F\alpha,0}$) are identifiable in addition to the original parameters (C_{PB}, $K^{i,j}$, $K_{0,\alpha_{J_g}}$, $K_{BS_{J_g}}$, and K_{BS_λ}). While it is unlikely that the effect of concentration on the steady-state air recovery would actually be linear, real-time parameter estimation could update this simple model to track the operating region of the system.

The fact that modelled frother concentrations are observable implies that such concentrations can be estimated without any concentration measurements. This is very promising as reagent concentrations in flotation plants are notoriously difficult to measure and on-line reagent concentration measuring techniques have yet to be developed (Gélinas and Finch, 2007; Maldonado et al., 2010). While Knight and Knights (2011) report some success with an on-line xanthate probe measuring the residual collector concentration, any such probe has yet to reach the market. The lack of such measurements makes any control strategy involving reagents very challenging. With concentration estimates, it is possible to include frother addition rate into a model-based control strategy.

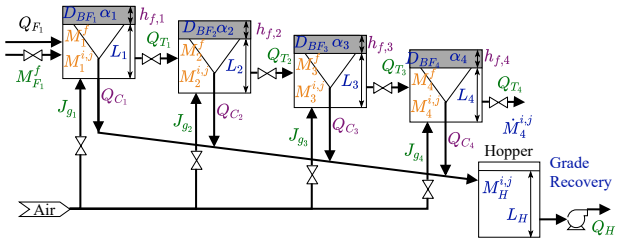

Fig. 1. Four-cell rougher circuit, described in Hadler et al. (2010), adapted from Oosthuizen et al. (2021). Green: manipulated variables. Blue: measured variables. Orange: variables not measured. Purple: intermediate variables.

5. SIMULATION

5.1 Simulation Set-up

The expanded models of Sections 4.1 and 4.2 were simulated using the variable values in Oosthuizen et al. (2021), as summarised in Table 2 and Table 3. The nominal values for the estimated parameters are given in Table 1. The bank of cells and most important variables are shown in Fig. 1. A solids content of 444 kg/m^3 in the feed was assumed. This translates to a solids mass fraction of 35 wt%. To achieve a frother concentration in the slurry around a typical 10 ppm (mass basis) (Harris et al., 2013), a frother dosage of between 0.01 kg/m^3 and 0.02 kg/m^3 is required. An initial concentration of $C_k^f = 0.01$ kg/m^3 was chosen for all cells and the feed composition. Without data containing varying frother dosages, the parameters for the model expansions could not be fitted properly. Instead, their nominal values (see Table 3) were chosen such that the model steady-state remains the same as in Oosthuizen et al. (2021) for the chosen nominal concentration. The following simulation results should therefore only be interpreted qualitatively to determine whether the model expansions have predictive potential.

Each run was simulated for a process time of 60 min with step changes in $\dot{M}_{F_1}^f$ as shown in Fig. 2. As the cells are assumed to be well-mixed and there are no transport delays in the model, the concentration in all cells react immediately, albeit with dynamics which become slower as one progress down the bank. The first cell reaches its

Table 2. Initial values of model variables for the flotation cells and hopper (Oosthuizen et al., 2021)

Variable	Unit	Cell 1	Cell 2	Cell 3	Cell 4	Hopper
Model states						
α_k	–	0.21	0.19	0.14	0.10	–
D_{BF_k}	mm	1.83	1.54	1.91	1.43	–
L	m	1.28	1.28	1.28	1.28	1.00
$M_k^{0,0}$	kg	51.8	29.4	16.8	16.8	235.8
$M_k^{1,0}$	kg	5118	5118	5118	5118	82.5
M_k^f	kg	0.11	0.11	0.11	0.11	–
Manipulated variables						
J_{g_k}	mm/s	7.45	8.45	9.51	10.02	–
Q_{T_k}	m^3/h	729.3	728.1	727.4	726.4	3.6

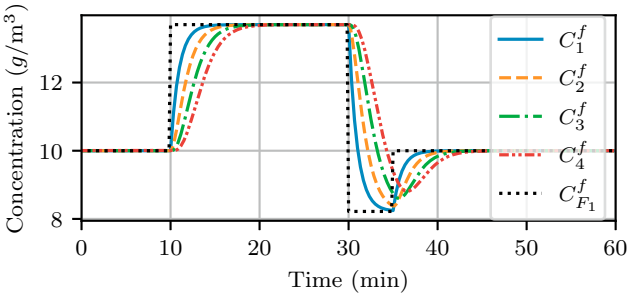

Fig. 2. Frother concentration in all cells with changes in frother addition rate.

steady-state concentration within 5 min, while the final cell takes about 10 min. The step durations mean that for the first step all cells reach steady-state, but that only Cell 1 is able to reach its steady-state value before the third step is implemented. The change in all other cells is interrupted by the third step. All further results are shown for Cell 4, as it has the slowest, most complex dynamics.

The models were simulated for three different constant pulp-levels, 1.28 m, 1.30 m, and 1.32 m, which correspond to froth heights of 120 mm, 100 mm, and 80 mm respectively. Henceforth, these simulations will be referred to as Runs 1, 2, and 3 for ME1, and Runs 4, 5, and 6 for ME2.

5.2 Model Expansion 1 (ME1) Results

An increase in froth stability is expected with higher frother concentrations, leading to higher air recoveries. However, during the ME1 simulation the calculated $K_{0,\alpha_{hf},k}$ is either larger or smaller than the froth height, depending on the simulation run, as shown in Fig. 3. ME1 incorrectly predicts an inversion in the effect of frother if the calculated $K_{0,\alpha_{hf},k}$ is larger than the froth height (see the simulation results in Fig. 4). This is especially clear in Run 2, where $K_{0,\alpha_{hf},k}$ moves past the froth height halfway through the response and the air recovery trajectory changes direction (compare Fig. 3 and Fig. 4)

5.3 Model Expansion 2 (ME2) Results

Next, consider the results for ME2 shown in Fig. 5. The direction of the frother effect is more in line with what is expected from literature (Wiese et al., 2011; Wills and Finch, 2015). Increasing the frother concentration improves the froth stability resulting in higher air recoveries. An increase in air recovery leads to an increase in mineral recovery and heights closer to the PAR height (94.9 mm) are shown to have higher air recoveries. This matches the observations of Hadler et al. (2012).

Table 3. Nominal values of model variables for the flotation bank

Variable	Unit	Value	Variable	Unit	Value
C_0^f	kg/m^3	0.01	$K_{F\alpha}$	–	3.0
$d_{p,\min}$	μm	2.77	$K_{F\alpha,0}$	–	0.01
$d_{p,\max}$	μm	23.2	$\dot{M}_{F_1}^f$	kg/h	7.3
K_{CF}	–	3000	Q_F	m^3/h	730.0
$K_{CF,0}$	–	64.9			

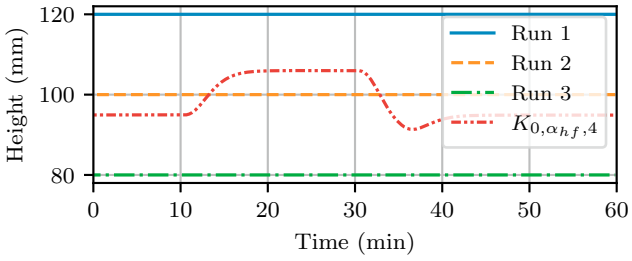

Fig. 3. Calculated $K_{0,\alpha_{hf},4}$ compared to the froth heights over the different simulation runs. Note that $K_{0,\alpha_{hf},4}$ crosses the froth height in Run 2, resulting in an opposite air recovery gradient.

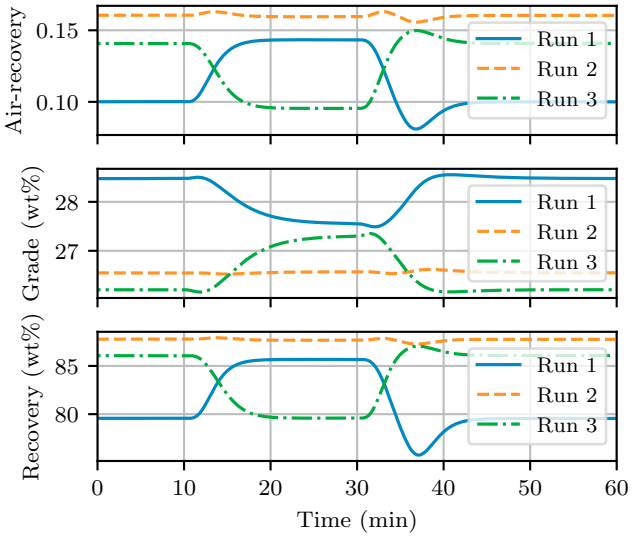

Fig. 4. Cell 4 results for the three simulations of ME1. Results show the incorrect inversion of frother effect.

Deeper froths result in higher grades due to an increase in drainage of entrained particles. Increased air recovery also leads to increased recovery through true flotation (see (1)). While more desired mineral is recovered through both mechanisms (drainage and true flotation), the increase in entrained gangue recovery causes the grade to decrease during periods with increased frother concentration.

The predicted magnitude of variation in air recovery, grade, and recovery is solely due to the specific model parameters chosen for the simulations. To obtain more realistic results and evaluate the predictive capabilities of the model expansion, industrial data is required. Most importantly, data is required where the frother concentration is varied.

6. CONCLUSION

The work presented here aims to serve as a proof of concept for the inclusion of reagent effect models in observable and identifiable dynamic modelling frameworks of froth flotation circuits. Of the two model expansions investigated, ME2 was found to be the most appropriate frother effect model. The fact that the concentrations can be estimated from the model without any concentration measurement

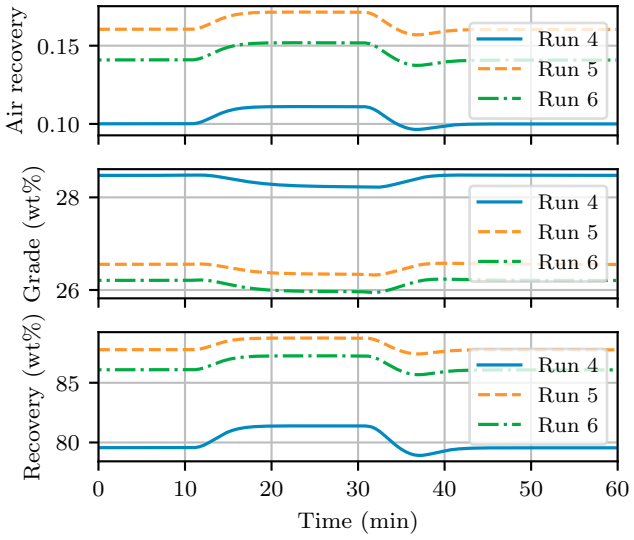

Fig. 5. Cell 4 results for the three simulation runs of ME2. Results show the model responding as expected.

is very promising indeed. Based on the results shown here, real time model-based control that includes reagent addition as a MV could be possible. Future work should include a sensitivity analysis using more appropriate variable ranges, as well as the validation and/or improvement of the model expansion. Both avenues rely heavily on obtaining plant data where the reagent dosage is varied. The current approach should also be expanded to consider the effect of the collector on the flotation parameters.

REFERENCES

Casali, A., Gonzalez, G., Agusto, H., and Vallebuona, G. (2002). Dynamic simulator of a rougher flotation circuit for a copper sulphide ore. *Minerals Engineering*, 15(4), 253–262.

Finch, J.A., Nesset, J.E., and na, C.A. (2008). Role of frother on bubble production and behaviour in flotation. *Minerals Engineering*, 21(12-14), 949–957.

Gélinas, S. and Finch, J.A. (2007). Frother analysis: some plant experiences. *Minerals Engineering*, 20(14), 1303–1308.

Hadler, K., Greyling, M., Plint, N., and Cilliers, J.J. (2012). The effect of froth depth on air recovery and flotation performance. *Minerals Engineering*, 36-38, 248–253.

Hadler, K., Smith, C.D., and Cilliers, J.J. (2010). Recovery vs. mass pull: The link to air recovery. *Minerals Engineering*, 23(11-13), 994–1002.

Harris, A., Venkatesan, L., and Greyling, M. (2013). A practical approach to plant-scale flotation optimization. *Journal of the Southern African Institute of Mining and Metallurgy*, 113(3).

Hermann, R. and Krener, A. (1977). Nonlinear controllability and observability. *IEEE Transactions on Automatic Control*, 22(5), 728–740.

Hodouin, D., Bazin, C., Gagnon, E., and Flament, F. (2000). Feedforward–feedback predictive control of a simulated flotation bank. *Powder Technology*, 108(2-3), 173–179.

Knight, J.W. and Knights, B.D.H. (2011). Industrial trial of Mintek's xanthoprobe at the Eland platinum concentrator. In *Proceedings of the 6th Southern African Base Metals Conference*, 87–98.

Maldonado, M., Desbiens, A., del Villar, R., and Aguilera, R. (2010). On-line estimation of frother concentration for flotation processes. *Canadian Metallurgical Quarterly*, 49(4), 435–446.

Neethling, S.J. and Cilliers, J.J. (2003). Modelling flotation froths. *International Journal of Mineral Processing*, 72(1-4), 267–287.

Neethling, S.J. and Cilliers, J.J. (2009). The entrainment factor in froth flotation: Model for particle size and other operating parameter effects. *International Journal of Mineral Processing*, 93(2), 141–148.

Oosthuizen, D.J., Craig, I.K., Jämsä-Jounela, S.L., and Sun, B. (2017). On the current state of flotation modelling for process control. *IFAC-PapersOnLine*, 50(2), 19–24.

Oosthuizen, D.J., Le Roux, J.D., and Craig, I.K. (2021). A dynamic flotation model to infer process characteristics from online measurements. *Minerals Engineering*, 167, 106878.

Putz, E. and Cipriano, A. (2015). Hybrid model predictive control for flotation plants. *Minerals Engineering*, 70, 26–35.

Quintanilla, P., Neethling, S.J., and Brito-Parada, P.R. (2021a). Modelling for froth flotation control: A review. *Minerals Engineering*, 162, 106718.

Quintanilla, P., Neethling, S.J., Navia, D., and Brito-Parada, P.R. (2021b). A dynamic flotation model for predictive control incorporating froth physics. Part I: Model development. *Minerals Engineering*, 173, 107192.

Saltelli, A., Annoni, P., Azzini, I., Campolongo, F., Ratto, M., and Tarantola, S. (2010). Variance based sensitivity analysis of model output. Design and estimator for the total sensitivity index. *Computer Physics Communications*, 181(2), 259–270.

Shean, B., Hadler, K., Neethling, S., and Cilliers, J.J. (2018). A dynamic model for level prediction in aerated tanks. *Minerals Engineering*, 125, 140–149.

Shean, B.J. and Cilliers, J.J. (2011). A review of froth flotation control. *International Journal of Mineral Processing*, 100(3-4), 57–71.

Steyn, C. and Sandrock, C. (2021). Causal model of an industrial platinum flotation circuit. *Control Engineering Practice*, 109, 104736.

Villaverde, A.F., Tsiantis, N., and Banga, J.R. (2019). Full observability and estimation of unknown inputs, states and parameters of nonlinear biological models. *Journal of The Royal Society Interface*, 16(156), 20190043.

Wang, L., Peng, Y., and Runge, K. (2017). The mechanism responsible for the effect of frothers on the degree of entrainment in laboratory batch flotation. *Minerals Engineering*, 100, 124–131.

Wiese, J., Harris, P., and Bradshaw, D. (2011). The effect of the reagent suite on froth stability in laboratory scale batch flotation tests. *Minerals Engineering*, 24(9), 995–1003.

Wills, B.A. and Finch, J. (2015). *Wills' Mineral Processing Technology: An Introduction to the Practical Aspects of Ore Treatment and Mineral Recovery*. Butterworth-Heinemann.